symmetry

MDPI

Review

Off-Shell Probes of the Higgs Yukawa Couplings: Light Quarks and Charm

Natascia Vignaroli

Dipartimento di Fisica "E. Pancini", Università di Napoli Federico II and INFN, Sezione di Napoli, Via Cinthia, 80126 Napoli, Italy; natascia.vignaroli@na.infn.it

Abstract: We review the present status and the future prospects for the measurements of the Higgs Yukawa couplings to light quarks and charm. A special focus is given to new proposed off-shell probes, which offer promising and complementary opportunities to test light quark Yukawas in triboson final states. Additionally, a new off-shell strategy to test the charm Yukawa coupling in the final state with two bosons plus a charm and a jet is considered. First estimates for the HL-LHC and the FCC-hh sensitivities on the channel are presented, showing encouraging results.

Keywords: Higgs; Yukawa couplings; charm; LHC; FCC

Citation: Vignaroli, N. Off-Shell Probes of the Higgs Yukawa Couplings: Light Quarks and Charm. *Symmetry* **2022**, *14*, 1183. https://doi.org/10.3390/sym14061183

Academic Editors: Theodota Lagouri and Alberto Ruiz Jimeno

Received: 19 May 2022
Accepted: 6 June 2022
Published: 8 June 2022

1. The Higgs Yukawa Couplings

The discovery of the Higgs boson at CERN 10 years ago [1,2] marked a breakthrough in our understanding of the physics of fundamental interactions, confirming the existence of the Brout–Englert–Higgs mechanism for the electroweak symmetry breaking (EWSB). However, it leaves us with unresolved questions in the standard model (SM), above all the non-explanation of the origin of the EWSB, the precarious nature of the associated potential, the unknown origin of the neutrino masses, the Higgs naturalness problem and the mysterious pattern of Yukawa couplings. The investigation of the properties of the Higgs, including its interactions, and in general of the EWSB sector is the primary objective of the LHC, which is approaching the upgrade to its high luminosity phase (HL-LHC) [3], as well as that of future planned experiments at the energy frontiers, e.g., the FCC [4–6], the ILC [7] or a multi-TeV muon collider [8]. ATLAS [9–12] (Figure 1) and CMS [13–15] measurements so far have given firm evidence of Higgs interactions to top, bottom and tau. The corresponding Yukawa couplings are measured with an accuracy of the order of 10% [9]. There was recently the first evidence for Higgs decay to muons [16,17], which represents the first probe of the Higgs interaction with the second generation of fermions and could give hints on scenarios beyond the SM (BSM) [18]. Crucial indication on the Higgs role in the mass generation of 1st and 2nd families would come from the challenging measurement of the light quark Yukawas. These are extremely difficult measurements but several techniques, which we are going to review, were recently developed to improve the detectability of the Higgs couplings to light quarks and to set bounds on possible deviations induced by physics beyond the SM. The current best constraints are placed by considering global fits to the Higgs strength, which is modified by shifts on the quark Yukawas (δy_q):

$$\mu = \frac{1}{1 + \sum_q (2\delta y_q + \delta y_q^2)\mathrm{Br}(h \to qq)_{\mathrm{SM}}} \tag{1}$$

where we are neglecting modifications to the Higgs production rate, since this would be affected only by $\delta y_q \gtrsim \mathcal{O}(10^3)$. Using the most recent measurements from CMS [19]

and ATLAS [20], respectively, $\mu = 1.06 \pm 0.07$ and $\mu = 1.02^{+0.07}_{-0.06}$, one can set the 95% C.L. bounds:

$$\begin{aligned} \delta y_d < 400\,, \delta y_u < 820\,, \delta y_s < 19 \quad \text{(ATLAS)} \\ \delta y_d < 450\,, \delta y_u < 930\,, \delta y_s < 22 \quad \text{(CMS)} \end{aligned} \tag{2}$$

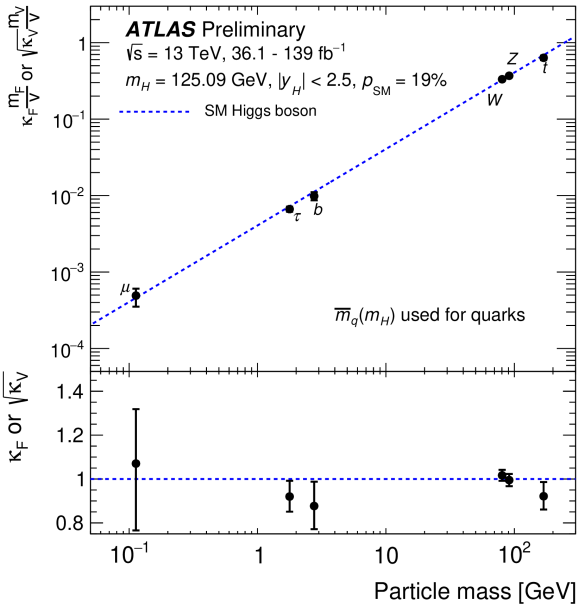

Figure 1. Measurements of Higgs Yukawa couplings confronted with the SM prediction. Plot extracted from the ATLAS study in Reference [9].

Considering the expectation for the high-luminosity LHC of measuring the total Higgs signal strength with an error of order 2–3% [3], these bounds from global fits could be improved up to

$$\delta y_d \lesssim 340\,, \delta y_u \lesssim 700\,, \delta y_s \lesssim 17 \quad \text{(HL-LHC)}. \tag{3}$$

Note that the different partonic content of the proton has a significant impact on the limits, and the improvement at HL-LHC might depend on the knowledge of the parton distribution functions (PDFs) at that time. Complementary alternative strategies have been proposed to test the light quark Yukawas. These include the study of rare Higgs decays into vector mesons, which gives limits $\delta y_q \lesssim 10^6$ [21], the analysis of the $W^\pm h$ charge asymmetry, with a sensitivity $\delta y_d \lesssim 1300$ [22] and, in particular, the study of the double Higgs production channel [23] and of the Higgs kinematics (p_T and rapidity) [24], which show competitive sensitivities with those from global fits at the HL-LHC:

$$\begin{aligned} \delta y_d \lesssim 850\,, \delta y_u \lesssim 1200 \quad \text{(double Higgs prod.)} \\ \delta y_d \lesssim 380\,, \delta y_u \lesssim 640 \quad \text{(Higgs kinematics)} \end{aligned} \tag{4}$$

All of these techniques represent *on-shell Higgs* probes. We instead discuss novel strategies which rely on the study of *off-shell Higgs* channels, following the idea of "measuring the Higgs couplings without the Higgs" [25]. The key observation behind this approach relies on the fact that modifications to the Higgs couplings affect the delicate cancellations, which avoid violation of perturbative unitarity at high energy in scatterings involving electroweak gauge bosons. This leads to measurable energy-growing effects.

2. Light Quark Yukawas in Triboson Final States

Modifications of light quark Yukawas lead to energy-growing effects in the *off-shell Higgs* triboson channel, which can be then analyzed to put constraints on δy_q. Figure 2 shows the leading tree-level Feynman diagrams contributing to the triple electroweak gauge boson channel, $q\bar{q} \to VVV$. In the SM, the Higgs exchange diagrams cancel the bad high-energy growing behavior of the remaining diagrams. Modifications of the Higgs Yukawa coupling spoil these delicate cancellations and lead to energy-growing amplitudes. We review the main results of the study in [26], which rely on this effect.

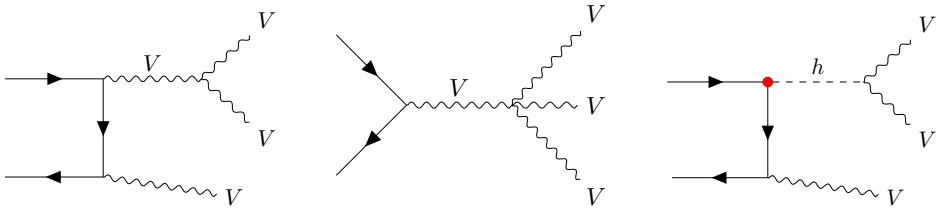

Figure 2. Feynman diagrams in the unitary gauge contributing to the triple electroweak gauge boson channel, $q\bar{q} \to VVV$.

The framework of the SM effective field theory (SMEFT) is adopted in [26]. In particular, this sub-set of dimension-6 gauge-invariant operators is assumed to encode the dominant BSM contribution to the Higgs Yukawa couplings to light quarks:

$$\mathcal{L}_{\text{SMEFT}} \supset -\frac{Y_u|H|^2}{v^2}\bar{u}_R Q_{1,L} H - \frac{Y_d|H|^2}{v^2}\bar{d}_R H^\dagger Q_{1,L} - \frac{Y_s|H|^2}{v^2}\bar{s}_R H^\dagger Q_{2,L} + \text{h.c.}\,, \tag{5}$$

where $Q_{1,L} = (u_L, d_L)$ and $Q_{2,L} = (c_L, s_L)$ represent the left-handed 1st and 2nd generation SM quark doublets, H is the Higgs doublet, and $v \approx 246$ GeV is the Higgs VEV. The parameters Y_q are assumed to be real, for simplicity. An example of a BSM scenario that can generate the operators in (5) is that of a new strong dynamics including a pseudo-Nambu–Goldstone composite Higgs [27] with decay constant f, where Higgs non-linearities can give shifts of the order v^2/f^2 to the Yukawa couplings. More in general, the operators in (5) can be generated by heavy vector-like quarks (also typically predicted in composite Higgs models) with masses of order $v/\sqrt{|Y_q|}$, which mix with the SM fermions after the EWSB.

Yukawa couplings are parametrized as

$$\mathcal{L} \supset -\frac{h}{v}\sum_{q=u,d,s} m_q(1+\delta y_q)\bar{q}q. \tag{6}$$

Modifications to the Yukawas with respect to the SM values are encoded in the parameters δy_q, which are related to the coefficients of the operators in Equation (5) by

$$\delta y_q = \frac{Y_q}{y_q^{\text{SM}}}\,. \tag{7}$$

Here, the SM Yukawa couplings are defined as $y_q^{\text{SM}} \equiv \sqrt{2}m_q/v$ (y_q^{SM} are evaluated at the Higgs mass scale).

The leading effect of the modification of the light quark Yukawas is manifested in the $q\bar{q} \to 3V_L$ channel. A clear picture of the effects induced by the BSM operators in (5) to the triboson process is obtained by adopting a non-unitary gauge description. The Higgs doublet can be then parametrized, introducing the would-be-Goldstone bosons G_i and the Higgs field h, as

$$H = \frac{1}{\sqrt{2}}\begin{pmatrix} i\sqrt{2}G_+ \\ v + h + iG_z \end{pmatrix}. \tag{8}$$

It is then easy to observe that the effective operators in (5) generate contact interactions between two quarks and three Goldstone bosons:

$$\begin{aligned}\mathcal{L} \supset & \frac{1}{v^2}\left(G_+G_- + \frac{1}{2}G_z^2\right)\left\{ iy_u^{\rm SM}\delta y_u\left(\sum_{q'=d,s}\bar{u}_R q'_L G_+ - \bar{u}_R u_L \frac{G_z}{\sqrt{2}}\right)\right. \\ & \left. + \; i\sum_{q'=d,s} y_{q'}^{\rm SM}\delta y_{q'}\left(\bar{q}'_R u_L G_- + \bar{q}'_R q'_L \frac{G_z}{\sqrt{2}}\right) + \text{h.c.}\right\}. \end{aligned} \tag{9}$$

These interactions characterize the $\mathcal{M}(q\bar{q} \to GGG)$ amplitudes which, by virtue of the equivalence theorem [28], approximate the high-energy behavior of the $\mathcal{M}(q\bar{q} \to VVV)$ amplitudes. At high energies, $\sqrt{s} \gg m_Z$, the diagram in Figure 3 represents the dominant contribution to the triboson channel.

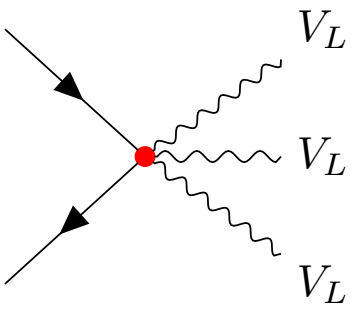

Figure 3. The Feynman diagram that gives, in the non-unitary gauge, the dominant contribution to the $\mathcal{M}(q\bar{q} \to GGG)$ amplitude at high energies. By virtue of the equivalence theorem $\mathcal{M}(q\bar{q} \to GGG) \approx \mathcal{M}(q\bar{q} \to V_L V_L V_L)$ at $\sqrt{s} \gg m_Z$.

Simple analytic expressions can be derived for the cross sections of the $q\bar{q} \to GGG$ processes induced by the interactions in Equation (9):

$$\begin{aligned} \sigma(q\bar{q} \to G_z G_+ G_-) &= (y_q^{\rm SM}\delta y_q)^2 I(\hat{s}), \\ \sigma(q\bar{q} \to 3G_z) &= \frac{3}{2}(y_q^{\rm SM}\delta y_q)^2 I(\hat{s}), \\ \sigma(u\bar{q}' \to G_+ G_z G_z) + \sigma(q'\bar{u} \to G_- G_z G_z) &= \frac{1}{2}\left[(y_u^{\rm SM}\delta y_u)^2 + (y_{q'}^{\rm SM}\delta y_{q'})^2\right] I(\hat{s}), \\ \sigma(u\bar{q}' \to G_+ G_+ G_-) + \sigma(q'\bar{u} \to G_- G_- G_+) &= 2\left[(y_u^{\rm SM}\delta y_u)^2 + (y_{q'}^{\rm SM}\delta y_{q'})^2\right] I(\hat{s}), \\ I(\hat{s}) &\equiv \frac{\hat{s}}{6144\pi^3 v^4}, \end{aligned} \tag{10}$$

where $\sqrt{\hat{s}}$ is the center-of-mass energy of the parton-level quark-antiquark annihilation and $q = u, d, s, q' = d, s$. By the equivalence theorem, for $\sqrt{\hat{s}} \gg m_Z$, these cross sections are approximately equal to those for the parton-level triple EW gauge boson production, with the identification $G_\pm \to W_L^\pm$ and $G_z \to Z_L$. It is manifested from (10) the energy-growing behavior of the cross section for the triboson channel, for $\delta y_q \neq 0$. In particular

$$\sigma(q\bar{q} \to V_L V_L V_L) \sim \mathcal{O}\left(\delta y_q^2 \frac{\hat{s}}{v^4}\right). \tag{11}$$

Interestingly, the triboson production was recently measured for the first time at the LHC by CMS [29]. This shows the LHC potential to further probe this channel. The main features of the BSM δy_q signal are the growing with energy of the cross section, but also a peculiar final state, characterized by the hard emission of gauge bosons and by distinctive angular distributions. The study in [26] exploits these characteristics to isolate the BSM δy_q induced signals from the background. It is clear that this specific search would significantly benefit from increasing the center-of-mass energy. It is indeed an ideal case to be studied

at the energy frontier experiments, in particular at the FCC-hh. Table 1 shows the cross-section values at the HL-LHC and at the FCC-hh of the triboson production channels in the SM and for the BSM signals generated by the operators in Equation (5) and associated to modifications of down, up and strange Yukawa couplings. Cross sections are computed with `MadGraph5_aMC@NLO` [30], at the next-to-leading order (NLO) in QCD for the SM [31,32] and at LO for the BSM. The BSM signals are generated by using an UFO model [33], which is available at [34]. The study in [26] performs an analysis of different triboson channels and final states. The most efficient are the WWW channels in same-sign dilepton and trilepton final states. It is, however, important to consider a combined analysis of several triboson channels to increase the sensitivity and to possibly disentangle the different δy_q. For example, the study of the neutral ZZZ and ZW^+W^- channels could, in principle, distinguish between δy_u and δy_d. The analyses performed in [26] apply a set of cuts on several distinctive observables of the processes. In particular, as shown in Figure 4 for the WWW trilepton channel, the p_T of the leptons in the final states, the missing E_T, or the angular azimuthal separation between leptons in the final states are particularly efficient to distinguish the δy_q signals, which are characterized by harder final states and a peculiar angular kinematics, from the SM background. The search is then refined by performing a binned-likelihood shape analysis on the p_T distributions of the leading lepton. More details on the analysis can be found in [26]. Clearly, there is much room for improvement of this study by considering, for example, combined shape analyses on several interesting p_T, E_T and angular distributions. The final results are shown on Table 2. The HL-LHC sensitivities on δy_q from the analysis of the triboson channels are competitive with those from global fits to the Higgs data, with the possibility to test δy_d up to order 400. The sensitivities are greatly enhanced at the FCC-hh, which could probe δy_d up to order 30. This corresponds to testing new physics scale for the operators in (5) of the order of 10 (3) TeV at the FCC-hh (HL-LHC), as shown in Figure 5.

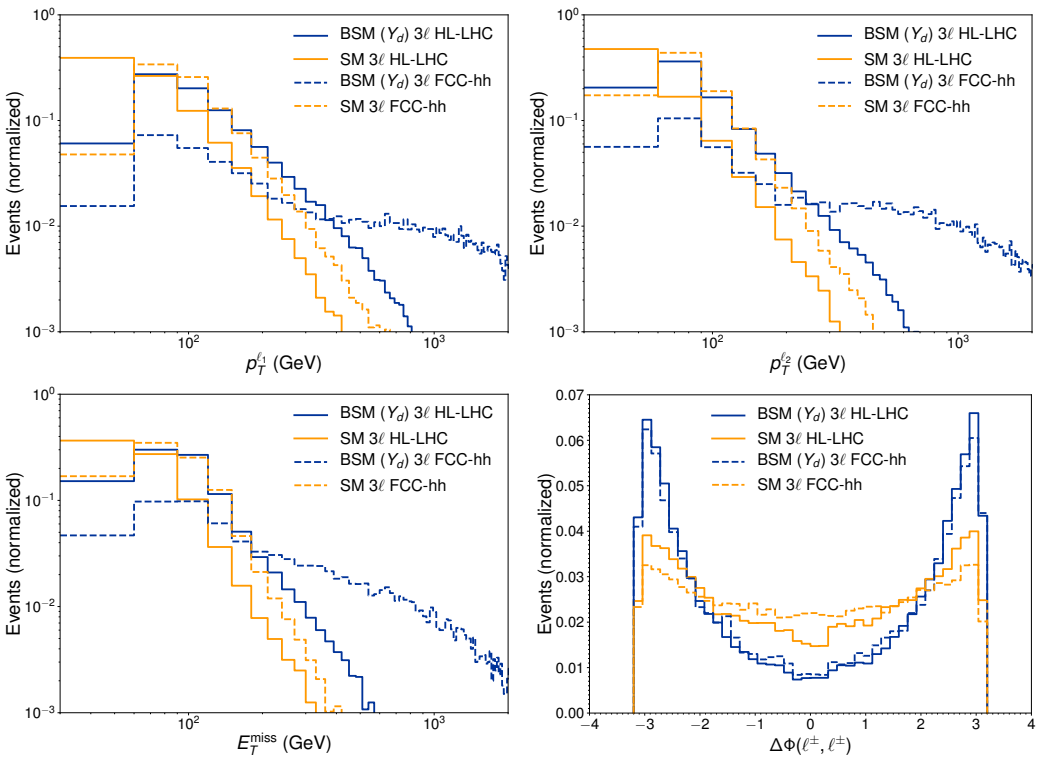

Figure 4. Differential distributions, normalized to unit area, for the WWW trilepton channel. Top-left: p_T of the leading-lepton. Top-right: p_T of the second-leading lepton. Bottom-left: E_T^{miss}. Bottom-right: the azimuthal separation $\Delta\Phi(\ell^\pm, \ell^\pm)$. The distributions for the pure BSM triboson signal are indicated by blue lines, those for the SM by yellow lines. Solid lines refer to the 14 TeV LHC, dashed ones to the 100 TeV FCC-hh.

Table 1. Cross-section values at the $\sqrt{s} = 14$ TeV LHC (upper table), and at the $\sqrt{s} = 100$ TeV FCC-hh (lower table) for different triboson production channels in the SM (computed at NLO in QCD) and for the BSM signals induced by the dimension-6 operators in Equation (5), with $Y_d = 1$ ($Y_{\neq d} = 0$), $Y_u = 1$ ($Y_{\neq u} = 0$) and $Y_s = 1$ ($Y_{\neq s} = 0$), respectively.

HL-LHC	**SM**	**BSM ($Y_d = 1$)**	**BSM ($Y_u = 1$)**	**BSM ($Y_s = 1$)**
$W^+W^-W^+$	152 fb	3.6 pb	3.6 pb	110 fb
$W^+W^-W^-$	87 fb	1.5 pb	1.5 pb	110 fb
ZZW^+	40 fb	1.0 pb	1.0 pb	31 fb
ZZW^-	23 fb	0.43 pb	0.43 pb	31 fb
ZW^+W^-	191 fb	1.5 pb	2.4 pb	120 fb
ZZZ	16 fb	0.99 pb	1.7 pb	66 fb
FCC-hh	**SM**	**BSM ($Y_d = 1$)**	**BSM ($Y_u = 1$)**	**BSM ($Y_s = 1$)**
$W^+W^-W^+$	2.35 pb	290 pb	290 pb	16 pb
$W^+W^-W^-$	1.76 pb	140 pb	140 pb	16 pb
ZZW^+	756 fb	74 pb	74 pb	4.4 pb
ZZW^-	579 fb	36 pb	36 pb	4.4 pb
ZW^+W^-	3.93 pb	94 pb	150 pb	12 pb
ZZZ	231 fb	110 pb	180 pb	11 pb

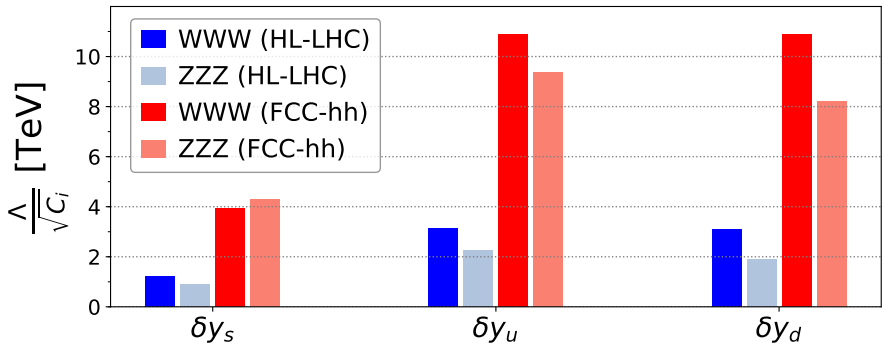

Figure 5. Main results from Reference [26]. HL-LHC (blue) and FCC-hh (red) projected 2σ reach, for different triboson channels, on the new physics scale Λ (with Wilson coefficient C_i) at which the dimension-6 Yukawa operators in (5) are generated.

Table 2. HL-LHC (FCC-hh) 2σ sensitivities on δy_q for the different sub-channels analyzed in [26].

	WWW			***ZZZ***		
	$\ell^\pm\ell^\pm + 2\nu + 2j$	$\ell^\pm\ell^\pm\ell^\mp + 3\nu$	**Comb.**	$4\ell + 2\nu$	$4\ell + 2j$	**Comb.**
δy_d	430 (36)	840 (54)	420 (34)	1500 (65)	1300 (93)	1100 (60)
δy_u	850 (71)	1700 (110)	830 (68)	2300 (100)	1800 (140)	1600 (92)
δy_s	150 (13)	230 (33)	140 (13)	300 (12)	290 (16)	250 (11)

3. Off-Shell Probe of the Charm Yukawa

We now focus on probing modifications to the Higgs Yukawa coupling of the charm by analyzing the *off-shell Higgs* channel with two gauge bosons plus a tagged charm and a jet in the final state: $VV + c + j$. The leading Feynman diagram, in the non-unitary gauge, is shown in Figure 6. In the case of the charm, this two-boson signal is enhanced, compared to the triboson channel considered in the previous section, by the larger parton distribution function, compared to the charm PDF, of the valence quark in the initial state. We show that

this off-shell probe is competitive with other on-shell strategies considered so far: the direct test of the $H \to c\bar{c}$ decay [35,36], possibly considering the associated Higgs production with a photon [37], the global fit to the Higgs signal strength [38], the indirect test via the radiative process $h \to J/\Psi + \gamma$ [39], the analysis of the Higgs plus charm channel [40] or the indirect probe from precision Higgs measurements [41]. These latter methods appear to be the most efficient, with the possibility to test, at the 95% C.L. at the HL-LHC, values

$$\begin{aligned} |\delta y_c| &\lesssim 2.6 \quad \text{(Higgs plus charm)} \\ |\delta y_c| &\lesssim 2.1 \quad \text{(Higgs precision measurements)} \end{aligned} \tag{12}$$

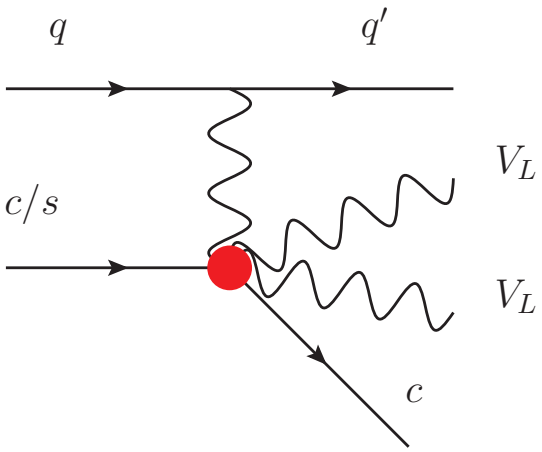

Figure 6. Leading Feynman diagram for the signal of modification to y_c in the non-unitary gauge. The red dot denotes the effective coupling (Equation (14)).

Analogously to the analysis for the triboson channel, we consider modification to the charm Yukawa

$$\delta y_c = \frac{Y_c}{y_c^{\text{SM}}} \tag{13}$$

induced by the following dim-6 operator

$$\mathcal{L}_{\text{SMEFT}} \supset -\frac{Y_c |H|^2}{v^2} \bar{c}_R Q_{1,L} H + \text{h.c.} \tag{14}$$

We assume Y_c to be a real parameter. As for the case discussed in the previous section, this operator spoils the mechanism of cancellation by the Higgs exchange of the energy-growing diboson amplitudes and leads to $\left(\delta y_c^2 \frac{\hat{s}}{v^4}\right)$ energy enhancement effects, analogous to those described in Equations (10) and (11). The BSM contribution can be estimated by considering an expansion of the inclusive cross section in the terms SM ($Y_c = 0$), plus the SM-BSM interference term, which is linear in the coefficient Y_c, plus the pure BSM term, which is quadratic in Y_c:

$$\sigma \approx \sigma^{\text{SM}}(Y_c = 0) + Y_c\, \sigma^{\text{INT}}(Y_c = 1) + Y_c^2\, \sigma^{\text{BSM}}(Y_c = 1)\,. \tag{15}$$

We find the cross-section values in the different $VVcj$ channels reported in Table 3. Calculations were made with `MadGraph5_aMC@NLO` at LO in QCD by using the UFO model available at [34]. Note that, differently from the previous case of the modifications to the light quark Yukawas, the interference term here is not negligible. This, as we will show, can give an handle to the possibility to test the sign of the modification to the charm Yukawa.

Table 3. Values of different $VVcj$ cross sections for $\sqrt{s} = 14$ TeV LHC (upper table) and $\sqrt{s} = 100$ TeV FCC-hh (lower table) for the SM and with the addition of the dimension-6 operator from Equation (14), with $Y_c = 1$. We show the cross section for the interference term and the purely BSM quadratic term. Calculations are at LO in QCD, and a minimum requirement $p_T\,(j), (c) > 20$ GeV is applied.

HL-LHC	**SM ($Y_c = 0$)**	**INT ($Y_c = 1$)**	**BSM ($Y_c = 1$)**
W^+W^-cj	2.3 pb	0.58 pb	63 pb
W^+Zcj	0.86 pb	0.17 pb	17 pb
W^-Zcj	0.79 pb	0.09 pb	9.1 pb
$ZZcj$	0.19 pb	0.14 pb	15 pb
W^+W^+cj	29 fb	0.42 fb	94 fb
W^-W^-cj	23 fb	0.31 fb	90 fb
FCC-hh	**SM ($Y_c = 0$)**	**INT ($Y_c = 1$)**	**BSM ($Y_c = 1$)**
W^+W^-cj	92 pb	6.4 pb	660 pb
W^+Zcj	36 pb	1.8 pb	190 pb
W^-Zcj	35 pb	1.3 pb	130 pb
$ZZcj$	6.8 pb	1.6 pb	180 pb
W^+W^+cj	0.76 pb	2.8 fb	3.0 pb
W^-W^-cj	0.68 pb	3.2 fb	3.0 pb

At this point, one can derive an estimate of the HL-LHC and FCC-hh sensitivities by considering a naive evaluation of the reducible background, which will contribute to the total background in addition to the irreducible component given by the SM $VVcj$ process. In particular, we estimate the significance σ by applying a background rescaling factor B, which parametrizes the number of reducible background events as a factor of the SM $VVcj$ events:

$$\sigma = \frac{N_{SM+BSM} - N_{SM}}{\sqrt{N_{SM} + B \times N_{SM}}}\,. \tag{16}$$

By focusing only on the semileptonic final state, $\ell^{\pm}\nu$+c+X, and considering a c-tagging efficiency of 25% [35,36], we find the 1σ and the 2σ sensitivities on δy_c of the HL-LHC and of the FCC-hh in the $VVcj$ channel shown in Figure 7. Sensitivities are presented as functions of the reducible background rescaling factor B. In the hypothesis of a negligible (compared to the SM $VVcj$ process) reducible background, we find the sensitivities on δy_c as

$$\begin{aligned} \delta y_c &\lesssim 0.43\,(1\sigma) - 0.77\,(2\sigma) \qquad \text{(HL-LHC, } 2{\times}3 \text{ ab}^{-1}\text{)} \\ \delta y_c &\lesssim 0.12\,(1\sigma) - 0.23\,(2\sigma) \qquad \text{(FCC-hh, } 30 \text{ ab}^{-1}\text{)} \end{aligned} \tag{17}$$

$$\begin{aligned} -\delta y_c &\lesssim 3.1\,(1\sigma) - 3.4\,(2\sigma) \qquad \text{(HL-LHC, } 2{\times}3 \text{ ab}^{-1}\text{)} \\ -\delta y_c &\lesssim 2.8\,(1\sigma) - 2.9\,(2\sigma) \qquad \text{(FCC-hh, } 30 \text{ ab}^{-1}\text{)} \end{aligned} \tag{18}$$

We consider these estimates a useful and encouraging starting point for more refined analysis. Future studies could exploit for example, similarly to what was discussed for the triboson channels, the peculiar kinematic of the BSM process to better isolate its contribution from the background and minimize, in particular, the reducible component of the background. Our results indicate sensitivities on δy_c in the diboson channel which could be realistically below order 1 at the HL-LHC, thus competitive and complementary to other charm Yukawa probes, and of the order of 20% at the FCC-hh. Interestingly, there is also the possibility to test the sign of δy_c, since, because of interference effects, the significance

is higher in the case of a positive shift to the charm Yukawa. Negative shifts of the order of $3y_c^{\mathrm{SM}}$ can be probed in the $VVcj$ channel.

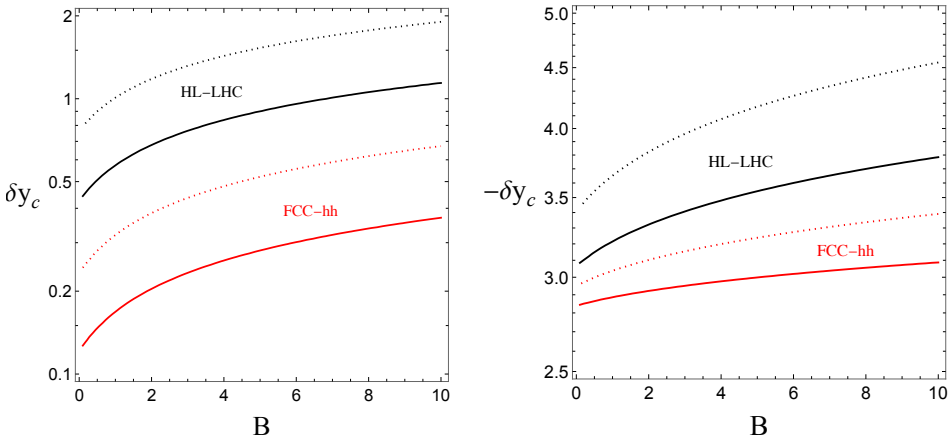

Figure 7. 1σ (continuous curve) and $2\,\sigma$ (dotted curve) HL-LHC (14 TeV, 2×3 ab^{-1}) and FCC-hh (100 TeV, 30 ab^{-1}) sensitivities on δy_c in the $VVcj$ channel and semileptonic final state, as functions of an arbitrary amount of reducible background, calculated as a factor B of the irreducible background given by the SM signal (cfr. Equation (16)).

4. Conclusions

The investigation of the properties of the Higgs boson, and in particular of its interactions and Yukawa couplings to SM fermions, is of primary importance for the understanding of high-energy physics. A crucial indication of the Higgs role in the mass generation of 1st and 2nd families comes from the measurement of the light quark Yukawas. We reviewed a novel technique to improve this challenging test based on the study of the triboson channel, where the Higgs is off-shell. In this approach, the Yukawa couplings are determined indirectly by their contributions via virtual Higgs exchange to the triboson process. This method relies on the fact that modifications of the Higgs Yukawas disturb the structure of the SM and lead to the violation of perturbative unitarity at high energy. The study of the triboson channel gives results that are competitive and complementary to other on-shell Higgs probe. In particular, the HL-LHC could test modification to the down (up) quark, δy_d (δy_u), up to order 400 (800). The sensitivities are greatly enhanced at the FCC-hh, which could probe δy_d (δy_u) up to order 30 (70). We then considered an off-shell Higgs probe of the charm Yukawa. In this case, we focused on the channel $VVcj$. First estimates of the HL-LHC and FCC-hh sensitivities, presented in Figure 7, indicate encouraging results and offer a useful starting point for more refined analyses at the LHC. Our first naive estimates indicate sensitivities on δy_c in the diboson channel, which could be realistically below order 1 at the HL-LHC, thus competitive and complementary to other charm Yukawa probes, and of the order of 20% at the FCC-hh. Interestingly, there is also the possibility to test the sign of the shift in the charm Yukawa.

Funding: This research received no external funding.

Informed Consent Statement: Not applicable.

Data Availability Statement: Not applicable.

Acknowledgments: The author thanks A. Falkowski, S. Ganguly, P. Gras, J. M. No, K. Tobioka, T. You, M. Son and E. Venturini for discussions and collaboration in the related studies [26,42], and in particular K. Tobioka for enligthing discussions on the possibility to test the charm Yukawa in the $VVcj$ channel.

Conflicts of Interest: The author declares no conflict of interest.

References

1. Aad, G.; Abajyan, T.; Abbott, B.; Abdallah, J.; Khalek, S.A.; Abdelalim, A.A.; Abdinov, O.; Aben, R.; Abi, B.; Abolins, M.; et al. Observation of a new particle in the search for the Standard Model Higgs boson with the ATLAS detector at the LHC. *Phys. Lett. B* **2012**, *716*, 1–29. [CrossRef]
2. CMS Collaboration; Chatrchyan, S. Observation of a New Boson at a Mass of 125 GeV with the CMS Experiment at the LHC. *Phys. Lett. B* **2012**, *716*, 30–61. . [CrossRef]
3. Cepeda, M.; Gori, S.; Ilten, P.; Kado, M.; Riva, F.; Khalek, R.A.; Aboubrahim, A.; Alimena, J.; Alioli, S.; Alves, A.; et al. Report from Working Group 2: Higgs Physics at the HL-LHC and HE-LHC. *CERN Yellow Rep. Monogr.* **2019**, *7*, 221–584. [CrossRef]
4. The FCC Collaboration. FCC Physics Opportunities: Future Circular Collider Conceptual Design Report Volume 1. *Eur. Phys. J. C* **2019**, *79*, 474. [CrossRef]
5. Michael, B.; Alain, B.; Olivier, B.; Mar, C.G.; Francesco, C.; Johannes, G.; Patrick, J.; Miguel, J.J.; Volker, M.; Attilio, M.; et al. FCC-ee: The Lepton Collider: Future Circular Collider Conceptual Design Report Volume 2. *Eur. Phys. J. ST* **2019**, *228*, 261–623. [CrossRef]
6. FCC Collaboration. FCC-hh: The Hadron Collider: Future Circular Collider Conceptual Design Report Volume 3. *Eur. Phys. J. ST* **2019**, *228*, 755–1107. [CrossRef]
7. Behnke, T.; Brau, J.E.; Foster, B.; Fuster, J.; Harrison, M.; Paterson, J.M.; Peskin, M.; Stanitzki, M.; Walker, N.; Yamamoto, H. The International Linear Collider Technical Design Report—Volume 1: Executive Summary. *arXiv* **2013**, arXiv:1306.6327.
8. Stratakis, D.; Mokhov, N.; Palmer, M.; Pastrone, N.; Raubenheimer, T.; Rogers, C.; Schulte, D.; Shiltsev, V.; Tang, J.; Yamamoto, A.; et al. A Muon Collider Facility for Physics Discovery. *arXiv* **2022**, arXiv:2203.08033.
9. Aad, G.; Abbott, B.; Abbott, D.C.; Abud, A.A.; Abeling, K.; Abhayasinghe, D.K.; Abidi, S.H.; AbouZeid, O.S.; Abraham, N.L.; Abramowicz, H.; et al. Combined measurements of Higgs boson production and decay using up to 139 fb^{-1} of proton-proton collision data at $\sqrt{s} = 13$ TeV collected with the ATLAS experiment. *Phys. Rev. D* textbf2020, *101*, 012002. [CrossRef]
10. ATLAS Collaboration. Measurements of Higgs boson production cross-sections in the $H \to \tau^+\tau^-$ decay channel in pp collisions at $\sqrt{s} = 13$ TeV with the ATLAS detector. *arXiv* **2022**, arXiv:2201.08269.
11. ATLAS Collaboration. Measurement of the associated production of a Higgs boson decaying into b-quarks with a vector boson at high transverse momentum in pp collisions at $\sqrt{s} = 13$ TeV with the ATLAS detector. *Phys. Lett. B* **2021**, *816*, 136204. [CrossRef]
12. ATLAS Collaboration. Evidence for the associated production of the Higgs boson and a top quark pair with the ATLAS detector. *Phys. Rev. D* **2018**, *97*, 072003. [CrossRef]
13. CMS Collaboration. Measurements of $t\bar{t}H$ Production and the CP Structure of the Yukawa Interaction between the Higgs Boson and Top Quark in the Diphoton Decay Channel. *Phys. Rev. Lett.* **2020**, *125*, 061801. [CrossRef]
14. CMS Collaboration. Measurement of Higgs Boson Production and Decay to the $\tau\tau$ Final State; CMS-PAS-HIG-18-032. 2019. Available online: https://cds.cern.ch/record/2668685 (accessed on 7 June 2022).
15. CMS Collaboration. Observation of Higgs boson decay to bottom quarks. *Phys. Rev. Lett.* **2018**, *121*, 121801. [CrossRef]
16. The ATLAS Collaboration. A search for the dimuon decay of the Standard Model Higgs boson with the ATLAS detector. *Phys. Lett. B* **2021**, *812*, 135980. [CrossRef]
17. Sirunyan, A.M.; Tumasyan, A.; Adam, W.; Bergauer, T.; Dragicevic, M.; Erö, J.; Valle, A.E.D.; Frühwirth, R.; Jeitler, M.; Krammer, N.; et al. Evidence for Higgs boson decay to a pair of muons.*J. High Energy Phys.* **2021**, *1*, 148. [CrossRef]
18. Vignaroli, N. Searching for a dilaton decaying to muon pairs at the LHC. *Phys. Rev. D* **2009**, *80*, 095023. [CrossRef]
19. CMS Collaboration. Combined Higgs Boson Production and Decay Measurements with up to 137 fb^{-1} of Proton-Proton Collision Data at $\sqrt{s}$ = 13 TeV; Tech. Rep. CMS-PAS-HIG-19-005. 2020. Available online: https://cds.cern.ch/record/2706103 (accessed on 7 June 2022).
20. ATLAS Collaboration. A Combination of Measurements of Higgs Boson Production and Decay Using Up to 139 fb^{-1} of Proton–Proton Collision Data at $\sqrt{s} = 13$ TeV Collected with the ATLAS Experiment; No. PUBDB-2020-05116. LHC/ATLAS Experiment. 2020. Available online: https://cds.cern.ch/record/2789544 (accessed on 7 June 2022).
21. Kagan, A.L.; Perez, G.; Petriello, F.; Soreq, Y.; Stoynev, S.; Zupan, J. Exclusive Window onto Higgs Yukawa Couplings. *Phys. Rev. Lett.* **2015**, *114*, 101802. [CrossRef]
22. Yu, F. Phenomenology of Enhanced Light Quark Yukawa Couplings and the $W^{\pm}h$ Charge Asymmetry. *J. High Energy Phys.* **2017**, *2*, 083. [CrossRef]
23. Alasfar, L.; Lopez, R.C.; Gröber, R. Probing Higgs couplings to light quarks via Higgs pair production.*J. High Energy Phys.* **2019**, *11*, 088. [CrossRef]
24. Soreq, Y.; Zhu, H.X.; Zupan, J. Light quark Yukawa couplings from Higgs kinematics. *J. High Energy Phys.* **2016**, *12*, 045. [CrossRef]
25. Henning, B.; Lombardo, D.; Riembau, M.; Riva, F. Measuring Higgs Couplings without Higgs Bosons. *Phys. Rev. Lett.* **2019**, *123*, 181801. [CrossRef] [PubMed]
26. Falkowski, A.; Ganguly, S.; Gras, P.; No, J.M.; Tobioka, K.; Vignaroli, N.; You, T. Light quark Yukawas in triboson final states. *J. High Energy Phys.* **2021**, *4*, 023. [CrossRef]
27. Agashe, K.; Contino, R.; Pomarol, A. The Minimal composite Higgs model. *Nucl. Phys. B* **2005**, *719*, 165–187. [CrossRef]
28. Lee, B.W.; Quigg, C.; Thacker, H.B. Weak Interactions at Very High-Energies: The Role of the Higgs Boson Mass. *Phys. Rev. D* **1977**, *16*, 1519. [CrossRef]
29. CMS Collaboration. Observation of the Production of Three Massive Gauge Bosons at $\sqrt{s}$ =13 TeV. *Phys. Rev. Lett.* **2020**, *125*, 151802. [CrossRef]

30. Alwall, J.; Frederix, R.; Frixione, S.; Hirschi, V.; Maltoni, F.; Mattelaer, O.; Shao, H.S.; Stelzer, T.; Torrielli, P.; Zaro, M. The automated computation of tree-level and next-to-leading order differential cross sections, and their matching to parton shower simulations. *J. High Energy Phys.* **2014**, *7*, 79. [CrossRef]
31. Dittmaier, S.; Huss, A.; Knippen, G. Next-to-leading-order QCD and electroweak corrections to WWW production at proton-proton colliders. *J. High Energy Phys.* **2017**, *9*, 034. [CrossRef]
32. Binoth, T.; Ossola, G.; Papadopoulos, C.G.; Pittau, R. NLO QCD corrections to tri-boson production. *J. High Energy Phys.* **2008**, *6*, 082. [CrossRef]
33. Degrande, C.; Duhr, C.; Fuks, B.; Grellscheid, D.; Mattelaer, O.; Reiter, T. UFO—The Universal FeynRules Output. *Comput. Phys. Commun.* **2012**, *183*, 1201–1214. [CrossRef]
34. Vignaroli, N. Effective Model for Modifications to Higgs Yukawa Couplings. Available online: https://feynrules.irmp.ucl.ac.be/wiki/YqHEFT (accessed on 7 June 2022).
35. ATLAS Collaboration. Prospects for $H \to c\bar{c}$ Using Charm Tagging with the ATLAS Experiment at the HL-LHC; ATL-PHYS-PUB-2018-016. 2018. Available online: http://cds.cern.ch/record/2633635 (accessed on 7 June 2022).
36. Han, T.; Nachman, B.; Wang, X. Charm-quark Yukawa Coupling in $h \to c\bar{c}\gamma$ at LHC. *Phys. Lett. B* **2019**, *793*, 90–96. [CrossRef]
37. Carlson, B.; Han, T.; Leung, S.C.I. Higgs boson to charm quark decay in vector boson fusion plus a photon. *Phys. Rev. D* **2021**, *104*, 073006. [CrossRef]
38. Perez, G.; Soreq, Y.; Stamou, E.; Tobioka, K. Constraining the charm Yukawa and Higgs-quark coupling universality. *Phys. Rev. D* **2015**, *92*, 033016. [CrossRef]
39. Bodwin, G.T.; Petriello, F.; Stoynev, S.; Velasco, M. Higgs boson decays to quarkonia and the $H\bar{c}c$ coupling. *Phys. Rev. D* **2013**, *88*, 053003. [CrossRef]
40. Brivio, I.; Goertz, F.; Isidori, G. Probing the Charm Quark Yukawa Coupling in Higgs+Charm Production. *Phys. Rev. Lett.* **2015**, *115*, 211801. [CrossRef]
41. Coyle, N.M.; Wagner, C.E.M.; Wei, V. Bounding the charm Yukawa coupling. *Phys. Rev. D* **2019**, *100*, 073013. [CrossRef]
42. Brooijmans, G.; Buckley, A.; Caron, S.; Falkowski, A.; Fuks, B.; Gilbert, A.; Murray, W.J.; Nardecchia, M.; No, J.M.; Torre, R.; et al. Les Houches 2019 Physics at TeV Colliders: New Physics Working Group Report. *arXiv* **2002**, arXiv:2002.12220.